Search for mSUGRA SUSY in the Like-Sign Dimuon Channel

A. Yurkewicz, R. Hauser, J. Linnemann, and R. Moore
D0 Note 4408

May 24, 2004

Abstract

We describe the search for the production of $\tilde{\chi}_1^{\pm}$ and $\tilde{\chi}_2^0$ particles. In gravity-mediated SUSY models, these particles may decay promptly to produce a tri-lepton final state which would be observable in a hadron collider environment. By requiring two like-sign leptons, the signal acceptance can be increased while maintaining a low background. We use this approach in analyzing dimuon events using 147 ± 10 pb^{-1} from the DØ Run II data set.

Contents

1 Introduction

Supersymmetry (SUSY) is a proposed symmetry between fermions and bosons [1]. If this symmetry exists, it is clearly broken as we only see half of the particle spectrum. One model which provides a simple breaking mechanism is called minimal supergravity (mSUGRA) SUSY. We perform a search for supersymmetry within this framework. A clean final state predicted by supersymmetric models is a tri-lepton final state from chargino and neutralino decays.

We search for these events by requiring like-sign (LS) dimuon pairs. Requiring only two muons increases the signal acceptance. Adding the like-sign requirement reduces the Standard Model background from Drell-Yan dimuon pairs and the various resonances in the dimuon spectrum. It has been suggested that the reach into some parts of mSUGRA parameter space will be greater when searching with the like-sign dilepton final state than the trilepton final state [2].

The like-sign dilepton final state results after the production of the $\tilde{\chi}_1^{\pm}$ and $\tilde{\chi}_2^0$. The $\tilde{\chi}_1^{\pm}$ can decay as

$$\tilde{\chi}_1^{\pm} \rightarrow \tilde{\chi}_1^0 + \mathrm{W}\ ; \qquad \mathrm{W} \rightarrow \mathrm{l} + \nu$$

or

$$\tilde{\chi}_1^{\pm} \rightarrow \nu + \tilde{l}; \qquad \tilde{l} \rightarrow \mathrm{l} + \tilde{\chi}_1^0.$$

The $\tilde{\chi}_2^0$ can decay as

$$\tilde{\chi}_2^0 \rightarrow \tilde{\chi}_1^0 + \mathrm{Z}; \qquad \mathrm{Z} \rightarrow \mathrm{l}+\mathrm{l}$$

or

$$\tilde{\chi}_2^0 \rightarrow \mathrm{l} + \tilde{l}; \qquad \tilde{l} \rightarrow \mathrm{l} + \tilde{\chi}_1^0.$$

Some points in mSUGRA parameter space that lead to final states with soft leptons (for example, when the chargino-slepton mass difference is small) may only be accessible through a search using the like-sign dilepton final state.

Combining the like-sign dilepton channels with the trilepton channels will provide increased sensitivity in the search for supersymmetry.

2 Data Set

We analyze data reconstructed with p14 versions of the d0reco package. The sample we use for our search is the common sample group dimuon skim [5, 6]. It is composed of events with two loose muons and no trigger requirement. It has all the standard DØ object corrections applied, and allows access to the certified objects. We remove events in our sample from runs marked as bad by the muon, jet/met, smt, or cft groups. We also remove luminosity blocks marked as bad by the luminosity group, or identified by the calorimeter group as being affected by the "ring-of-fire" problem [3], as these events will have mismeasured MET and isolation. Up to run 174306, we require the trigger 2MU_A_L2M0 to have fired. From run 174307 on, we require the trigger 2MU_A_L2ETAPHI to have fired. After removing these runs and luminosity blocks, the total integrated luminosity of the data sample passing one of our triggers is 147 ± 10 pb^{-1}.

2.1 Muon Selection Criteria

For this analysis, we use reconstructed muons that satisfy the following criteria (see Reference [4] for more information about certified muons):

- Identified by the muon id group as at least loose quality.
- Passed cosmic-ray-removal cuts: time between scintillator hits between -10 and 10 ns. Measured distance of closest approach to primary vertex less than 0.16 cm.
- Parameter nseg equal to 3 (the muon has stubs in the A and BC layers, plus a match to a central track).
- Matched to central track which is not an axial-only track.
- Matched to central track with at least one SMT hit.

2.2 Muon Isolation Definition

In this analysis, we wish to reject muons produced in association with jets. These muons constitute a large background, mainly from $b\overline{b}$, and muons from our signal should be produced in decays not involving jets. We refer to muons not produced in association with jets as isolated muons.

To be considered isolated, a muon must satisfy the requirements suggested in Reference [7]:

- The energy measured in the calorimeter in the annulus between 0.1 and 0.4 centered around the muon must be less than 2.5 GeV.
- The scalar sum of the transverse momenta of all tracks (except the one matched to the muon) contained within a cone of radius 0.5 around the muon must be less than 2.5 GeV/c.

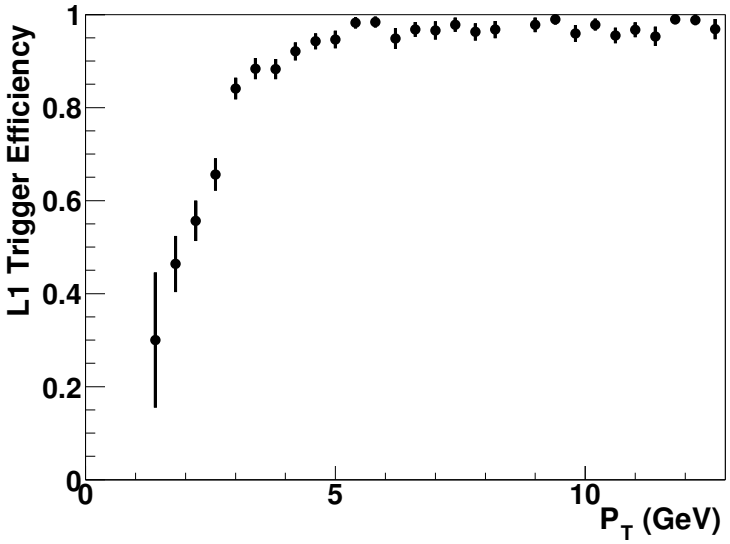

Figure 1: The L1 trigger efficiency as a function of p_T with respect to loose, nseg = 3 muons.

3 Trigger Efficiency

The triggers used in this analysis were 2MU_A_L2M0 and 2MU_A_L2ETAPHI. They have the same requirement at Level 1(L1); at least two muons using only the scintillating tiles. At Level 2(L2), the triggers differ. 2MU_A_L2M0 requires one L2 medium muon, while 2MU_A_L2ETAPHI requires two L2 medium muons, separated in η or ϕ. The separation requirement is a small one imposed only to avoid triggering on duplicate muons.

The per-muon trigger efficiencies were calculated with respect to reconstructed muon defined in section 2.1 as a function of η, ϕ, and p_T at L1 and L2.

3.1 L1 Muon Efficiency

We use dimuon events from the common sample group 1MU skim that fired a single muon trigger. We randomly pick a "control muon," which is matched in space to a L1 trigger object. The other muon is then the test muon, and we know whether or not it would have fired the trigger by checking whether there is a matching L1 muon object. We can then determine the per-muon L1 efficiency as a function of the reconstructed muon p_T, η, and ϕ.

Figure 1 shows the L1 muon efficiency versus p_T measured with respect to loose, nseg = 3 (track-matched) muons. The efficiency versus η is plotted in Figure 2 for muons with p_T greater than 5 GeV/c.

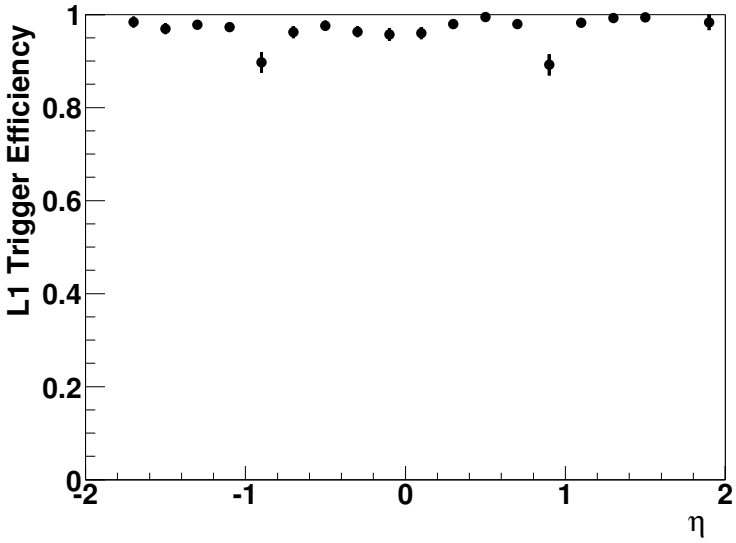

Figure 2: The L1 trigger efficiency as a function of η with respect to loose, nseg = 3 muons with p_T greater than 5 GeV/c.

3.2 L2 Muon Efficiency

We can use dimuon events that passed the L1 dimuon trigger to measure the L2 trigger efficiency. We ask that the control muon be matched to a L2 muon. Then we check whether the test muon has a L2 muon match. We can determine the per-muon L2 efficiency as a function of reconstructed muon p_T, η, and ϕ. The L2 efficiency versus η is plotted in Figure 3.

3.3 Total Trigger Efficiency

We apply the L1 and L2 efficiencies to all Monte Carlo samples. Since two different triggers were used, the total efficiencies were slightly different for the two run ranges. We apply the two efficiencies in proportion to the amount of data collected with each.

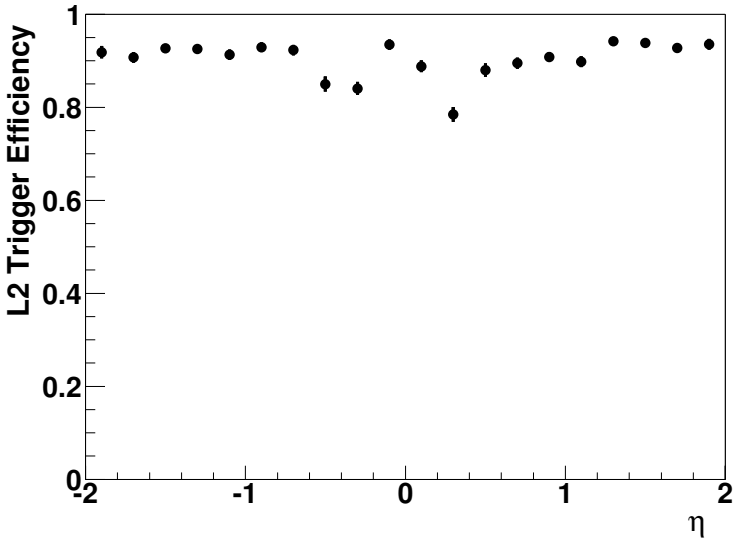

Figure 3: The L2 trigger efficiency as a function of η with respect to loose, nseg = 3 muons with p_T greater than 5 GeV/c.

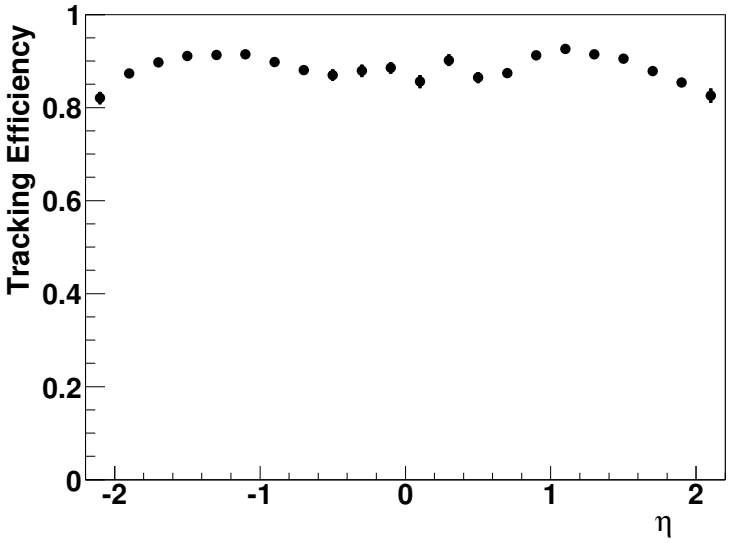

Figure 4: The tracking efficiency as a function of η with respect to local muons in the J/Ψ peak.

4 Reconstruction Efficiencies and Smearing

The discrepancy between data and Monte Carlo reconstruction efficiency must be determined so that the Monte Carlo can be corrected and used to simulate the data properly.

While the per-muon trigger efficiency can be determined with respect to the reconstructed muons, there is no analogous reference muon for a reconstructed muon. The total muon reconstruction efficiency can be measured, however, by separating it into the product of the local muon efficiency and the tracking efficiency.

4.1 Tracking Efficiency

We can calculate the tracking efficiency by selecting a high-purity dimuon sample. Events that fired one of our triggers are chosen. One muon is chosen randomly as the control muon. It is required to have a matched track, and be matched to L1 and L2 muons. The other muon is the test muon, and we only look at the local muon system information. We form the invariant mass between the pairs, and choose pairs whose invariant mass is in the J/Ψ region (2.0–4.0 GeV/c^2), a region where real muons should dominate backgrounds. We measure how often tracks are matched to the local muons. Figures 4 and 5 show the tracking efficiency as a function of η in data and Monte Carlo. Figure 6 shows the ratio of these efficiencies.

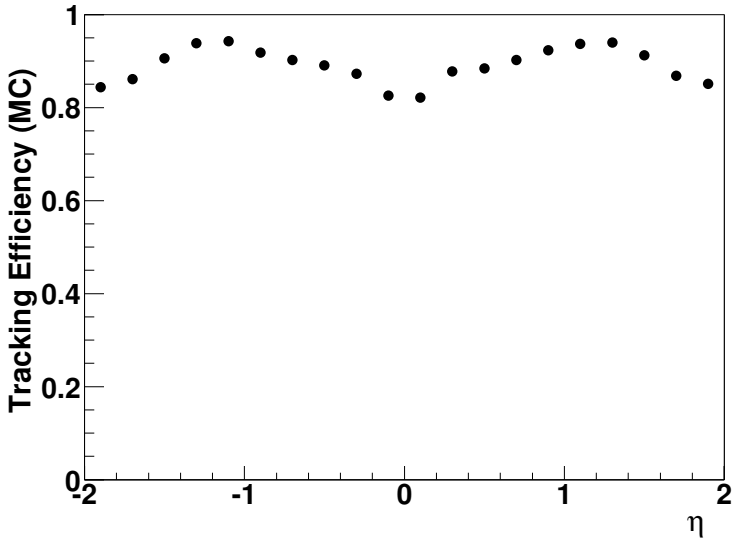

Figure 5: The tracking efficiency as a function of η with respect to Monte Carlo muons.

4.2 Local Muon Efficiency

We measure the muon detector's efficiency as above by again selecting a dimuon sample with one muon matched to a track (and a L1 and L2 muon), and one track where we don't look at the muon system information. We require that the invariant mass be in the Z region, and study how often a muon is matched to the track. The single muon skim is used to avoid a bias from using the dimuon skim. We also require a single muon trigger to have fired. Figures 7 and 8 show the loose muon efficiency as a function of η in data and Monte Carlo. Figure 9 shows the ratio of these efficiencies. A small correction is applied to the Monte Carlo to remove the discrepancy.

4.3 Muon Reconstruction Efficiency

The muon reconstruction efficiency is obtained by combining the reconstruction and tracking efficiencies. This efficiency is plotted as a function of η in Figure 10.

4.4 Monte Carlo Momentum Smearing

The muon p_T resolutions in data and Monte Carlo do not agree. In order to correct the difference, we smear the Monte Carlo p_T according to the prescription:

$$\frac{1}{p_T} \rightarrow \frac{A}{p_T} + fG \tag{1}$$

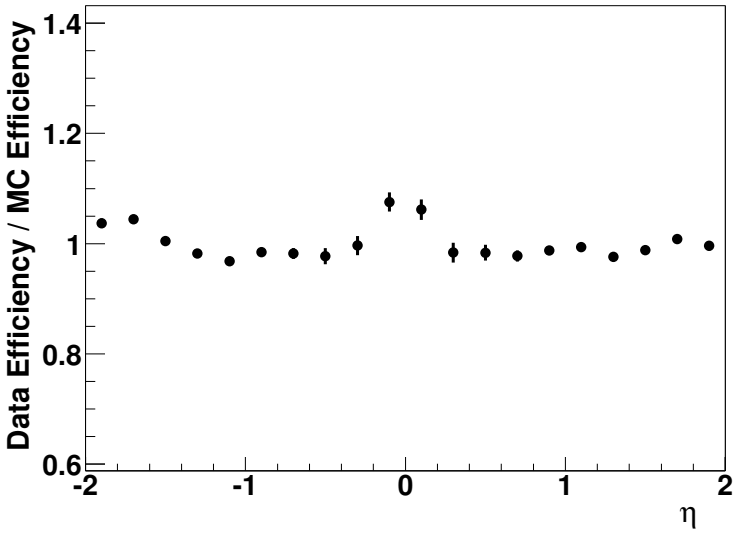

Figure 6: The data tracking efficiency divided by the Monte Carlo tracking efficiency as a function of η with respect to local muons in the J/Ψ peak.

where A = 1.0, f = 0.002, and G is a random number from a Gaussian distribution with width 1 and mean 0. The smearing values were determined by comparing Z Monte Carlo and data.

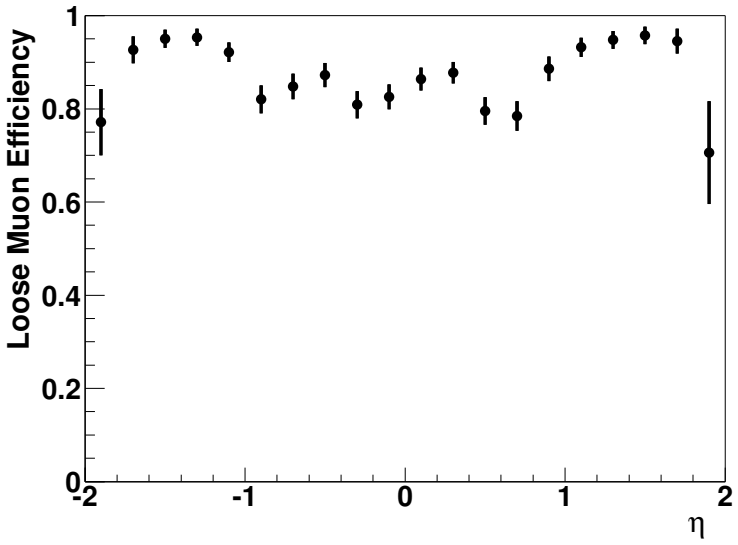

Figure 7: The loose muon efficiency as a function of η with respect to tracks measured in data. The tracks are from muon-track pairs with an invariant mass that lies under the Z peak.

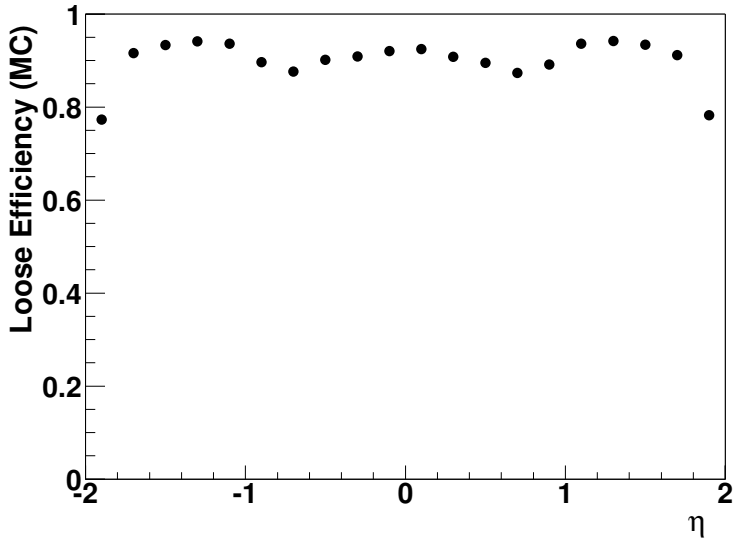

Figure 8: The loose muon efficiency as a function of η with respect to Monte Carlo muons.

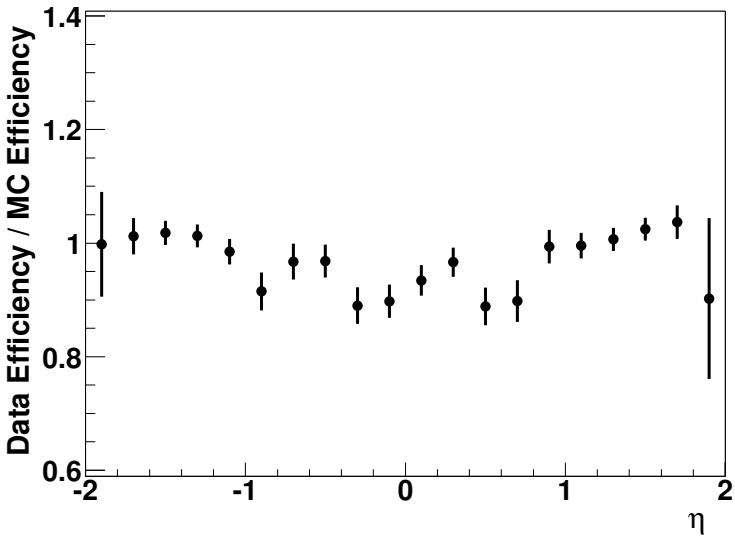

Figure 9: The data local muon efficiency divided by the Monte Carlo local muon efficiency as a function of η with respect to local muons in the Z peak.

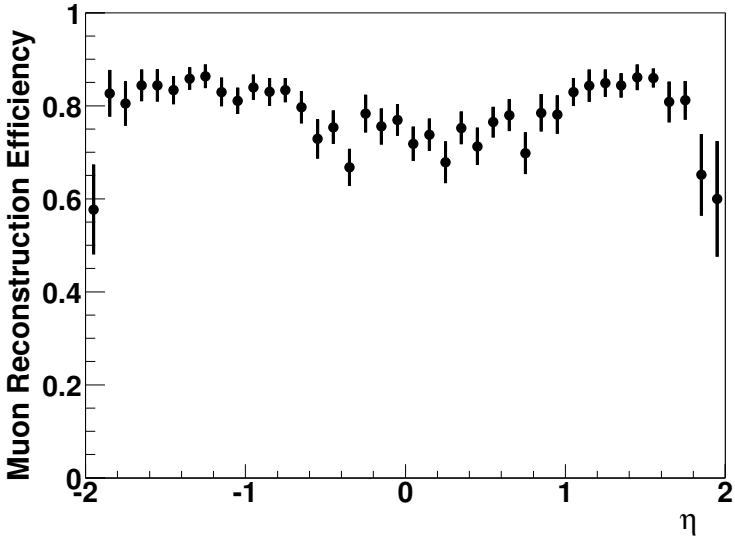

Figure 10: The total muon reconstruction efficiency as a function of η.

Sample	*MC Cross Section* (pb)	*Number of MC Events*	*Integrated Luminosity* (pb^{-1})
$t\bar{t}$	0.07	1250	18382
W+1 jet	757.6	115000	151.8
W+2 jets	222.1	46000	207.1
WZ	2.5	16500	6600
ZZ	1.1	15000	13393
Wbb	1.54	32000	20779
Zbb	0.24	96500	402083

Table 1: Table showing the sizes, calculated cross sections, and integrated luminosities for the various Monte Carlo (MC) samples generated.

5 Background

Not many Standard Model processes are capable of generating a pair of isolated like-sign muons. The physics background processes that we consider are $t\bar{t}$, $b\bar{b}/c\bar{c}$, W+jets, and di-boson production (WZ and ZZ). We modeled these backgrounds with Monte Carlo samples, with the exception of the $b\bar{b}/c\bar{c}$ sample.

Table 1 lists the Monte Carlo samples used. In addition to the backgrounds listed above, Drell-Yan, Z, and Upsilon (1s and 2s) samples were used for some studies. A k-factor of 1.33 was used to correct the leading-order cross section for the Drell-Yan and Z samples [8].

The PYTHIA event generator and the full DØ simulation and reconstruction software chain were used.

We apply the trigger and reconstruction efficiencies from Sections 3 and 4. For the $b\bar{b}/c\bar{c}$ background, we rely on an estimate from the data (see Section 5.1).

5.1 Background from $b\bar{b}/c\bar{c}$

We expect the largest source of like-sign dimuon pairs to be $b\bar{b}$ and $c\bar{c}$ production. The ideal strategy would be to generate a Monte Carlo sample to model this background, as we do with all other backgrounds. This technique was tried in the past. There are several problems. First, the angular distribution plots made from the data and Monte Carlo do not agree. This is most likely due to missing $b\bar{b}$ production mechanisms in the Monte Carlo. Second, the error on the cross section is large due to a disagreement between the measured and theoretically predicted cross sections. Finally, the large $b\bar{b}$ cross section makes the production of the desired luminosity difficult. This leads to a large error on the background estimate. This problem will worsen as our data set grows.

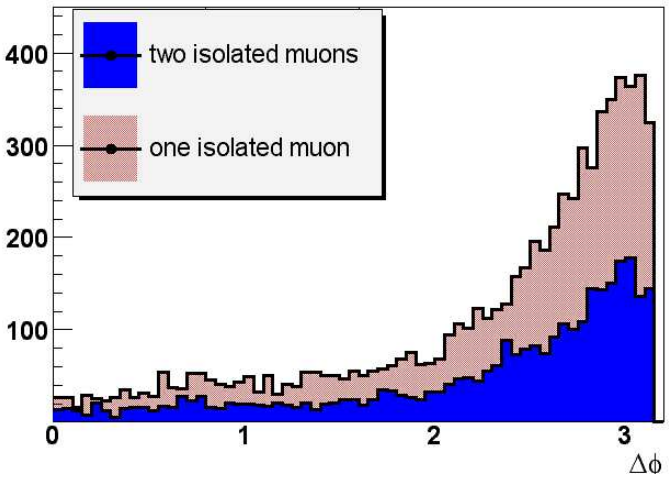

Figure 11: $\Delta\phi$ between two muons.

In lieu of Monte Carlo, we turn to the data for an estimate of the $b\overline{b}$ and $c\overline{c}$ background. Our method relies on finding a collection of events which contain muons similar to those that will be present in the sample in which we will look for our signal. We find this collection by looking for like-sign pairs of muons where one muon passes our isolation cuts, and one muon fails our isolation cuts by a small margin. The failing muon will be "nearly" isolated. That is, if a muon fails the isolation criteria by a small amount, it will resemble an isolated muon more closely than one that failed the criteria by a large amount. We choose the following definition of "nearly" isolated:

- The muon fails at least one of the isolation criteria defined in Section 2.2.
- The hollow cone energy must be less than 7 GeV.
- The p_T sum of all tracks within a cone of radius 0.5 must be less than 7 GeV/c.

The number of events in our nearly isolated sample must be scaled to the isolated sample to accurately predict the number of events. We do this by defining the ratio R:

$$R = \frac{\text{number of pairs with two isolated muons}}{\text{number of pairs with one isolated muon}} \tag{2}$$

.

We measure R in the region $\Delta\phi(\mu,\mu) > 2.7$, to avoid the bias of normalizing to our signal sample. This region is chosen because the $b\overline{b}/c\overline{c}$ background is peaked here, while the signal is flat (see Fig. 11). We then make the cut of $\Delta\phi(\mu,\mu) < 2.7$ one

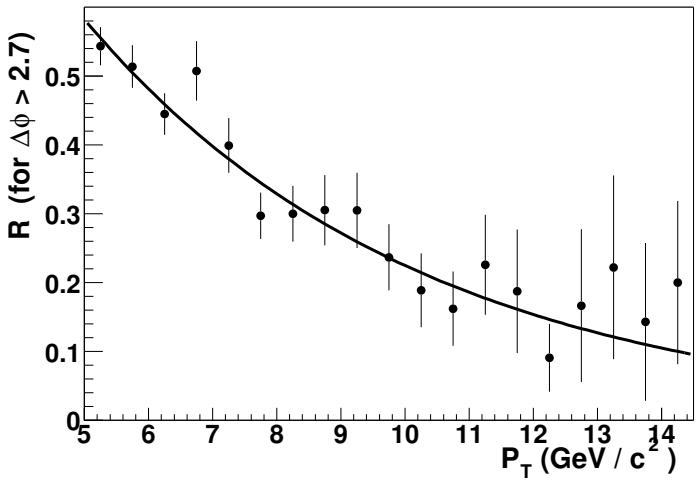

Figure 12: Ratio R (defined in the text) as a function of the p_T of the non-isolated muon.

of our final cuts on the data. Once we measure R, we can scale our nearly isolated sample by R, and use it to model our background.

We expect that R may be a function of the momentum of the muons in the like-sign pairs. Since most of the events in both of these samples come from B decays, the difference between those measured as isolated or nearly isolated is most likely due to the momentum kick the muon gets in the decay. Lower momentum muons may be kicked away from the B jet and hence measured as isolated more frequently than higher momentum muons. We observe this effect when measuring R as a function of p_T (Figure 12).

We measure R as a function of the p_T of the non-isolated muon by first calculating the number of events in each p_T bin in the nearly isolated and in the isolated sample. We then calculate R in each bin.

The correct way to measure R would be as a function of the p_T of the first and second muons in the pair. The statistics are not sufficient to do this. We have tried randomly choosing a muon from the two muons in the isolated sample, as well as using both muons and dividing by two. The results are similar with both methods.

We fit an exponential function to the distribution in Figure 12. We then scale (weight) the events in our nearly isolated sample, event-by-event, by the value of R corresponding to the p_T of the non-isolated muon belonging to the like-sign muon pair in that event. We are left with a sample of like-sign pairs of muons which should represent the isolated $b\overline{b}/c\overline{c}$ muons, and be scaled correctly to the like-sign, isolated sample which we are trying to describe.

Once we have this sample, we can test its ability to mimic isolated muons from $b\overline{b}/c\overline{c}$ by looking at the opposite-sign (OS) dimuon invariant mass distribution. The isolated

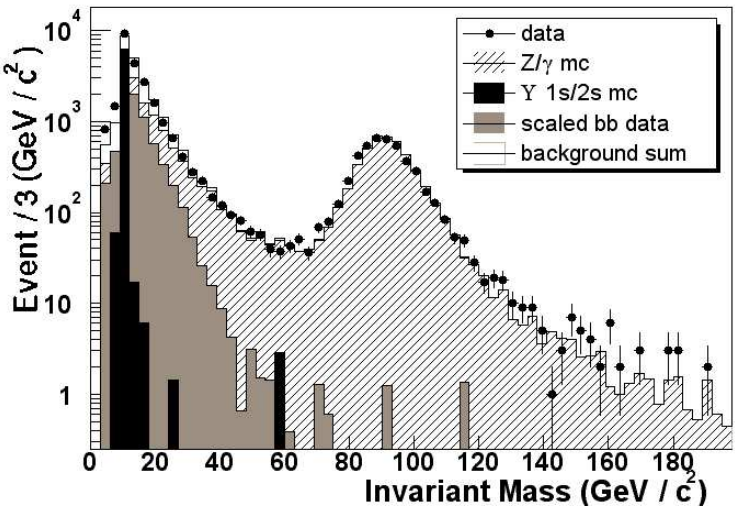

Figure 13: Circles show the invariant mass distribution of opposite-sign muon pairs. Backgrounds are described by the legend.

muons from $b\overline{b}/c\overline{c}$ contained in this sample should be similar to those in the like-sign sample. The normalization will be different. We first subtract the Drell-Yan, Z, and Upsilon backgrounds as predicted by the Monte Carlo from the opposite-sign distribution. We should be left with the opposite-sign, isolated muon pairs from $b\overline{b}/c\overline{c}$. We would like to compare our scaled, like-sign, nearly isolated sample to this one since they should be similar. The number of events in each sample will be different. We scale the like-sign, nearly isolated sample by the ratio of the number of entries remaining in the opposite-sign data sample to the number of events in the like-sign, nearly isolated sample. Figure 13 shows the opposite-sign, isolated data, and the various backgrounds. Figure 14 shows the invariant mass distribution in data after all backgrounds besides $b\overline{b}/c\overline{c}$ are subtracted, and the expected $b\overline{b}/c\overline{c}$, extracted from the like-sign data.

With this sample, we can model the $b\overline{b}/c\overline{c}$ background in our signal sample, and estimate the number of $b\overline{b}/c\overline{c}$ events given any set of cuts. Figure 15 shows the like-sign isolated data (the sample which may contain signal) compared to the estimation from the scaled nearly isolated sample.

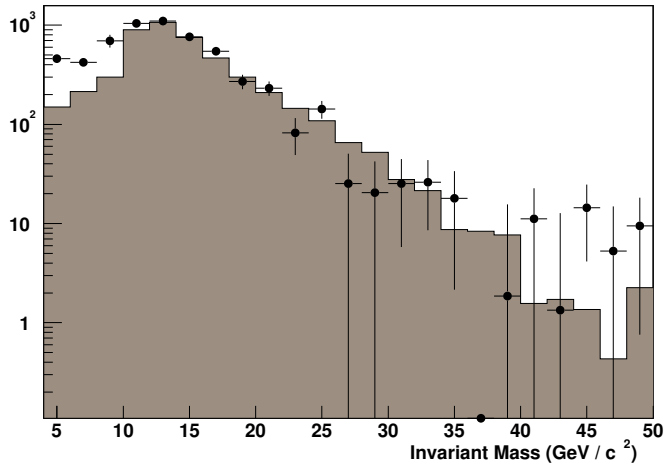

Figure 14: Circles show the invariant mass distribution of opposite-sign muon pairs after the subtraction of Monte Carlo background estimations. The shaded histogram is the expected remaining background, from $b\overline{b}/c\overline{c}$, which is estimated using like-sign data.

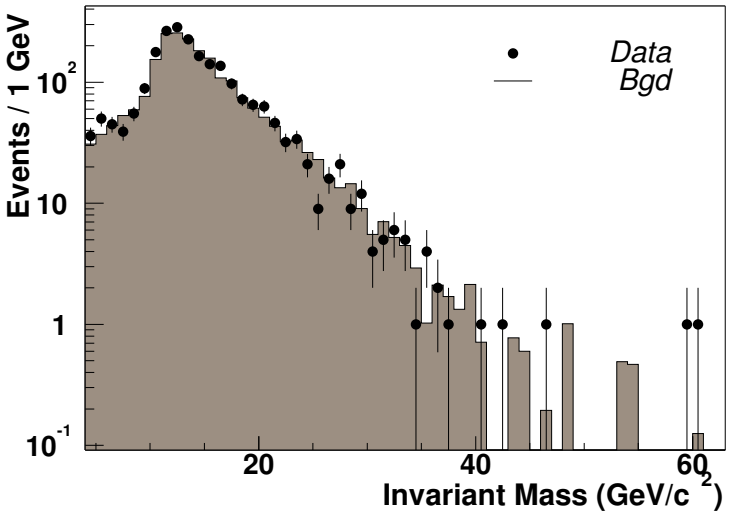

Figure 15: Circles show the invariant mass distribution of isolated like-sign muon pairs. This is the sample which may contain signal. The shaded histogram is the expected remaining background, from $b\overline{b}/c\overline{c}$, which is estimated using the nearly isolated like-sign data as described in the text.

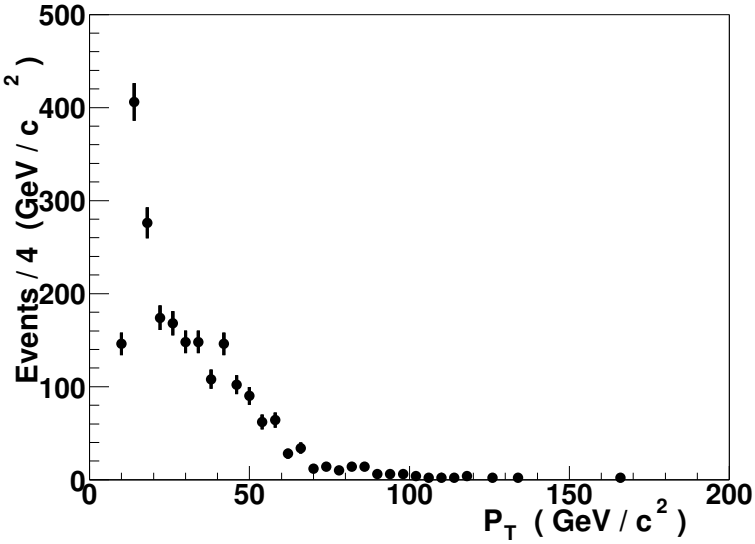

Figure 16: p_T spectrum of opposite-sign muon pairs in data. These muons could be used to estimate the pool of candidates for sign mismeasurement.

5.2 Sign Misidentification Background

Another source of like-sign dimuon pairs is an instrumental one. If the p_T of the muon is badly mismeasured, the charge assigned to the muon can be wrong. This can turn an opposite-sign pair into a like-sign pair. Since this analysis depends upon the proper determination of the sign of each muon, an estimate of the sign misidentification rate is necessary.

The sign misidentification rate is included in background estimates from Monte Carlo samples. The major source of sign misidentification comes from Z/γ events where one muon has its momentum badly mismeasured. The tables describing the number of events surviving each cut include the backgrounds from this source (labeled "Z/γ") as predicted by the Monte Carlo simulation.

As a check, like-sign pairs with each muon having a p_T greater than 15 GeV/c and with a phi difference greater than 2.8 can be chosen from the Z Monte Carlo and data. We expect these pairs to each contain a muon from a Z decay with its charge mismeasured. Although the statistics are low, there is reasonable agreement with 4 events in data and 3.4 events in Monte Carlo.

We also can attempt to crosscheck this estimate using data. The spectrum of opposite-sign pairs which form the pool of candidates for mismeasurement is plotted in Figure 16. This is a plot of all the muon pairs which fail the $\Delta\phi$ cut, and have a p_T greater than 11.0 GeV/c. This spectrum should be multiplied by the charge mismeasurement rate, if it can be obtained from data. To do this, we look at opposite-sign pairs of track-matched muons. We first choose one muon randomly. We use this muon's momentum as measured in the tracker. For the other muon, we use the mo-

mentum measured in the muon system. We then form the invariant mass of the pair. If the invariant mass is in the Z peak, we compare the sign measured in the muon system to the sign measured by the tracking system. We extract the rate of sign mismeasurement as a function of p_T.

Unfortunately, the invariant mass distribution did not show a clear Z peak. This is likely due to the poor momentum resolution of the muon system at high p_T. This crosscheck method is therefore not reliable.

Point	m_0	$m_{1/2}$	$\tan\beta$	*sign*(μ)	A_0	$\sigma \times BR$ (pb)
SUSY 1	68	182	3	+	0	0.59
SUSY 2	90	180	3	+	0	0.20
SUSY 3	85	190	5	+	0	0.40
SUSY 4	108	220	5	+	0	0.15
SUSY 5	65	170	5	+	0	0.83
SUSY 6	70	175	3	+	300	0.45
SUSY 7	75	180	3	+	300	0.38
SUSY 8	80	185	3	+	300	0.33
SUSY 9	85	190	3	+	300	0.28
SUSY 10	85	195	3	+	300	0.24
SUSY 11	90	200	3	+	300	0.20
SUSY 12	76	170	3	+	0	0.32
SUSY 13	80	175	3	+	0	0.25
SUSY 14	84	180	3	+	0	0.21
SUSY 15	65	180	3	+	300	0.58
SUSY 16	70	185	3	+	300	0.48
SUSY 17	75	190	3	+	300	0.37
SUSY 18	72	165	3	+	0	0.39
SUSY 19	74	168	3	+	0	0.35
SUSY 20	88	185	3	+	0	0.18

Table 2: Table showing the mSUGRA parameter values for the 13 SUSY points chosen to study.

6 Signal Monte Carlo

Eventually a full scan of the mSUGRA parameter space will be performed. For this note, only a few representative points are chosen. The points are summarized in Table 2.

We multiply these cross sections by a K-factor of 1.25 following [9].

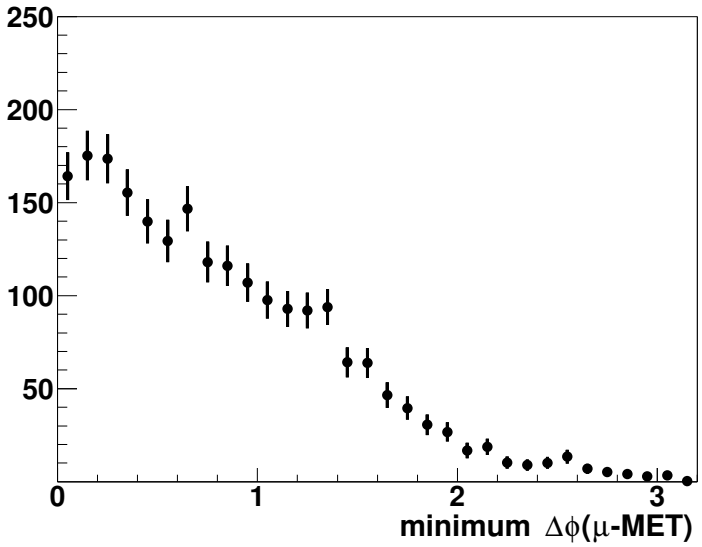

Figure 17: $\Delta\phi$ between MET and muon closer to MET.

7 Summary of Cuts

We start with the following basic selection:

- Events must have two loose, nseg = 3 (track-matched), like-sign muons.
- Both muons must be isolated.
- Both muons must have $p_T > 5$ GeV/c.

This defines our initial data set, part of which is used to predict the background as described in section 5. We then apply the following set of cuts:

- The distance in ϕ between the two muons must be less than 2.7.
- Leading muon $p_T > 11$ GeV/c.
- Missing $E_T > 15$ GeV/c.

- Invariant mass of opposite-sign muon pairs $M(\mu, \mu) < 70$ or > 110 GeV/c. This rejects background events containing Z, coming from WZ, ZZ and Z/γ.
- Invariant mass of like-sign muon pairs $M(\mu, \mu) < 80$ GeV/c. This rejects background events containing Z where a charge flip occurred for one of the muons.

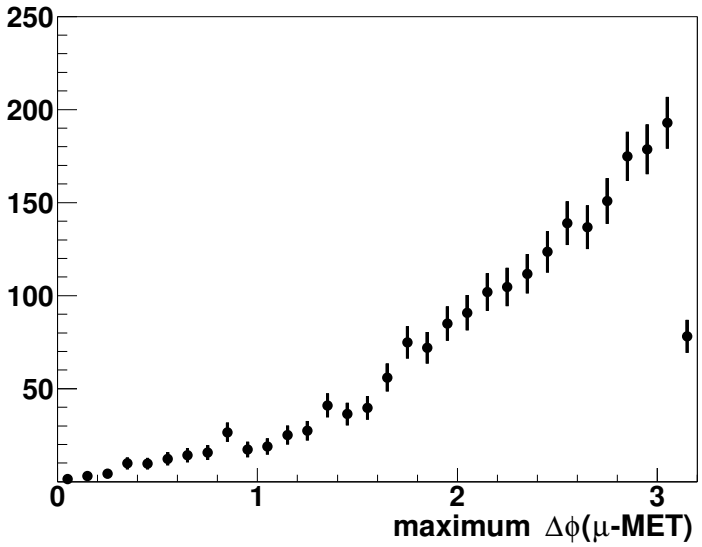

Figure 18: $\Delta\phi$ between MET and muon further away from MET.

If the second muon has a $p_T > 11$ GeV, we pass the event at this stage. Otherwise we look at the separation in ϕ between missing E_T and the muons, and missing E_T and jets. We call $\Delta\phi_{min}(MET, \mu)$ the separation between the muon closer to the MET, and $\Delta\phi_{max}(MET, \mu)$ the separation for the muon further away. We expect these low p_T events to come mostly from $b\overline{b}$ and have muons and jets aligned with MET from the neutrino.(see Fig. 17, 18, 19. We introduce a cut:

- $\Delta\phi_{min}(MET, \mu) > 0.5$ and $\Delta\phi_{max}(MET, \mu) < 2.4$.

If there are jets in the event, we look at the $\Delta\phi(Jet, MET)$ between the jet and the MET and apply a cut:

- $\Delta\phi(Jet, MET)) < 2.4$.

The last two cuts are only applied if the p_T of the second leading muon is less than 11 GeV.

The effect of these cuts on our background, signal Monte Carlo samples and data is shown in Tables 3,4,6, 7,8 and 11.

We see 1 event passing our cuts in the data where we expect 0.13±0.04 from the background.

There are several sources of error on the background estimation. The trigger and reconstruction efficiency measurements have estimated errors of less than 1%. The systematic errors from the uncertainty on the Monte Carlo cross sections are estimated at 10%.

Sample	$b\bar{b}$	wz	zz	$t\bar{t}$	wbb
Initial	2175 (30)	0.264 (0.062)	0.045 (0.018)	0.004 (0.004)	0.161 (.028)
$\Delta\phi(\mu,\mu)$	1209.6 (23)	0.203 (0.054)	0.037 (0.016)	0.004 (0.004)	0.120 (.025)
$p_T > 11$	57.8 (3.74)	0.203 (0.054)	0.037 (0.016)	0.004 (0.004)	0.120 (.025)
$MET > 15$	17.9 (2.01)	0.178 (0.051)	0.023 (0.013)	0.004 (0.004)	0.109 (.023)
$\Delta\phi(Jet, MET)$	3.2 (0.83)	0.167 (0.050)	0.023 (0.013)	0.004 (0.004)	0.005 (.005)
$\Delta\phi(\mu, MET)$	0.042 (0.03)	0.167 (0.050)	0.023 (0.013)	0.004 (0.004)	0.005 (.005)
LS InvMass	0.042 (0.03)	0.102 (0.038)	0.016 (0.011)	0	0.005 (.005)
OS InvMass	0.042 (0.03)	0.069 (0.031)	0.016 (0.011)	0	0.005 (.005)

Table 3: The number of events remaining after applying each cut to the background samples

Sample	zbb	wj	wjj	Z/γ (2-15)	Z/γ (15-60)
Initial	0.047 (.003)	2.1(1.2)	0	0	1.59 (1.12)
$\Delta\phi(\mu,\mu)$	0.040 (.003)	2.1(1.2)	0	0	1.59 (1.12)
$p_T > 11$	0.040 (.003)	2.1(1.2)	0	0	0.744 (0.744)
$MET > 15$	0.017 (.003)	2.1(1.2)	0	0	0
$\Delta\phi(Jet, MET)$	0.004 (.001)	0	0	0	0
$\Delta\phi(\mu, MET)$	0.002 (.001)	0	0	0	0
LS InvMass	0	0	0	0	0
OS InvMass	0	0	0	0	0

Table 4: Number of events after applying each cut to the background samples.

Sample	Z/γ (60-130)	Z/γ (130-250)
Initial	3.43 (0.638)	0.074 (0.024)
$\Delta\phi(\mu,\mu)$	0.902 (0.319)	0
$p_T > 11$	0.902 (0.319)	0
$MET > 15$	0.454 (0.227)	0
$\Delta\phi(Jet, MET)$	0.336 (0.194)	0
$\Delta\phi(\mu, MET)$	0.336 (0.194)	0
LS InvMass	0	0
OS InvMass	0	0

Table 5: Number of events after applying each cut to the background samples.

Sample	SUSY 1	SUSY 2	SUSY 3	SUSY 4
Initial	0.571 (0.043)	0.415 (0.022)	0.235 (0.021)	0.124 (0.009)
$\Delta\phi(\mu,\mu)$	0.463 (0.038)	0.326 (0.019)	0.163 (0.018)	0.099 (0.008)
$p_T > 11$	0.426 (0.036)	0.312 (0.019)	0.159 (0.018)	0.093 (0.008)
$MET > 15$	0.371 (0.050)	0.269 (0.030)	0.141 (0.022)	0.087 (0.011)
$\Delta\phi(Jet, MET)$	0.184 (0.035)	0.182 (0.029)	0.074 (0.016)	0.048 (0.009)
$\Delta\phi(\mu, MET)$	0.178 (0.038)	0.178 (0.034)	0.074 (0.016)	0.048 (0.010)
LS InvMass	0.172 (0.037)	0.161 (0.031)	0.064 (0.016)	0.036 (0.008)
OS InvMass	0.166 (0.036)	0.150 (0.029)	0.064 (0.016)	0.036 (0.008)

Table 6: Number of events after applying each cut to signal MC

Sample	SUSY 5	SUSY 6	SUSY 7	SUSY 8
Initial	0.428 (0.041)	0.583 (0.068)	0.532 (0.061)	0.335 (0.037)
$\Delta\phi(\mu,\mu)$	0.303 (0.035)	0.450 (0.059)	0.385 (0.052)	0.278 (0.033)
$p_T > 11$	0.240 (0.031)	0.439 (0.059)	0.360 (0.050)	0.274 (0.033)
$MET > 15$	0.202 (0.035)	0.434 (0.072)	0.317 (0.057)	0.246 (0.040)
$\Delta\phi(Jet, MET)$	0.086 (0.022)	0.274 (0.063)	0.198 (0.050)	0.202 (0.045)
$\Delta\phi(\mu, MET)$	0.086 (0.023)	0.274 (0.063)	0.198 (0.050)	0.202 (0.045)
LS InvMass	0.082 (0.022)	0.256 (0.063)	0.167 (0.045)	0.172 (0.040)
OS InvMass	0.082 (0.022)	0.256 (0.063)	0.167 (0.045)	0.159 (0.038)

Table 7: Number of events after applying each cut to signal MC

Sample	SUSY 9	SUSY 10	SUSY 11	SUSY 12	SUSY 13
Initial	0.332 (0.035)	0.359 (0.047)	0.310 (0.045)	1.009 (0.107)	0.713 (0.060)
$\Delta\phi(\mu,\mu)$	0.284 (0.032)	0.241 (0.038)	0.228 (0.038)	0.787 (0.084)	0.585 (0.055)
$p_T > 11$	0.280 (0.032)	0.235 (0.038)	0.214 (0.037)	0.744 (0.081)	0.571 (0.054)
$MET > 15$	0.259 (0.040)	0.192 (0.039)	0.201 (0.041)	0.658 (0.097)	0.475 (0.068)
$\Delta\phi(Jet, MET)$	0.189 (0.037)	0.123 (0.032)	0.157 (0.039)	0.423 (0.077)	0.323 (0.061)
$\Delta\phi(\mu, MET)$	0.189 (0.042)	0.123 (0.034)	0.157 (0.042)	0.420 (0.087)	0.312 (0.067)
LS InvMass	0.154 (0.035)	0.097 (0.029)	0.143 (0.039)	0.383 (0.080)	0.291 (0.063)
OS InvMass	0.154 (0.035)	0.097 (0.029)	0.143 (0.039)	0.368 (0.077)	0.291 (0.063)

Table 8: Number of events after applying each cut to signal MC

Sample	SUSY 14	SUSY 15	SUSY 16	SUSY 17
Initial	0.494 (0.047)	0.764 (0.098)	0.803 (0.099)	0.672 (0.081)
$\Delta\phi(\mu,\mu)$	0.404 (0.043)	0.637 (0.085)	0.611 (0.079)	0.478 (0.061)
$p_T > 11$	0.389 (0.042)	0.567 (0.078)	0.569 (0.075)	0.431 (0.056)
$MET > 15$	0.333 (0.051)	0.491 (0.085)	0.542 (0.090)	0.398 (0.066)
$\Delta\phi(Jet, MET)$	0.182 (0.039)	0.221 (0.050)	0.280 (0.059)	0.235 (0.049)
$\Delta\phi(\mu, MET)$	0.177 (0.042)	0.221 (0.055)	0.276 (0.065)	0.228 (0.052)
LS InvMass	0.159 (0.039)	0.203 (0.051)	0.255 (0.061)	0.203 (0.048)
OS InvMass	0.159 (0.039)	0.203 (0.051)	0.255 (0.061)	0.200 (0.047)

Table 9: Number of events after applying each cut to signal MC

Sample	SUSY 18	SUSY 19	SUSY 20
Initial	1.202 (0.131)	1.055 (0.115)	0.595 (0.064)
$\Delta\phi(\mu,\mu)$	0.944 (0.105)	0.837 (0.094)	0.464 (0.050)
$p_T > 11$	0.856 (0.097)	0.765 (0.086)	0.444 (0.049)
$MET > 15$	0.767 (0.116)	0.653 (0.099)	0.400 (0.059)
$\Delta\phi(Jet, MET)$	0.445 (0.083)	0.417 (0.077)	0.273 (0.050)
$\Delta\phi(\mu, MET)$	0.441 (0.094)	0.410 (0.087)	0.273 (0.057)
LS InvMass	0.396 (0.085)	0.380 (0.081)	0.254 (0.052)
OS InvMass	0.389 (0.083)	0.360 (0.077)	0.243 (0.051)

Table 10: Number of events after applying each cut to signal MC

Sample	Background	Data
Initial	2189.1 (31)	2275 (48)
$\Delta\phi(\mu,\mu)$	1216.6 (23)	1279 (36)
$p_T > 11$	63.9 (4.0)	47 (6.8)
$MET > 15$	20.8 (2.1)	16 (4)
$\Delta\phi(Jet, MET)$	3.74 (0.85)	4 (2)
$\Delta\phi(\mu, MET)$	0.58 (0.20)	1 (1)
LS InvMass	0.16 (0.06)	1 (1)
OS InvMass	0.13 (0.06)	1 (1)

Table 11: Number of events in data and expected from the sum of all backgrounds after applying each cut.

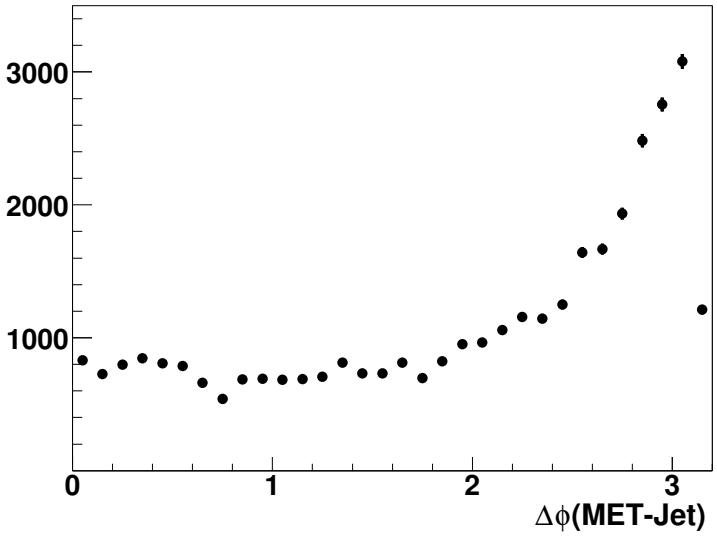

Figure 19: $\Delta\phi(MET, Jet)$ for all jets.

There are also systematic errors arising from differences between the Monte Carlo and data in the MET, $\Delta\phi_{min}(MET, \mu)$, $\Delta\phi_{max}(MET, \mu)$, and $\Delta\phi(MET, Jet)$ distributions. We check the difference in predicting the number of events passing this cut in Monte Carlo and data by comparing Z Monte Carlo and data. We can see the percentage of events beyond the cut value in Monte Carlo and data and take the difference as an estimate of the systematic error. The errors are estimated at 10% for MET, 10% for $\Delta\phi_(MET, \mu)$, and 10% for $\Delta\phi(MET, Jet)$.

Three event displays of the event passing our cuts are shown in Figures 20, 21, and 22.

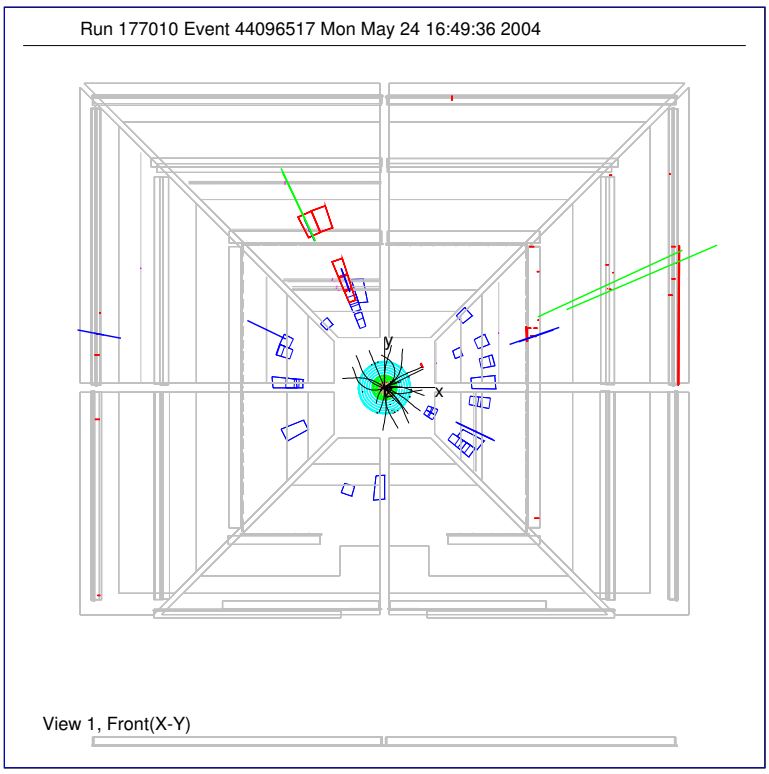

Figure 20: Event display of event 44096517 from run 177010.

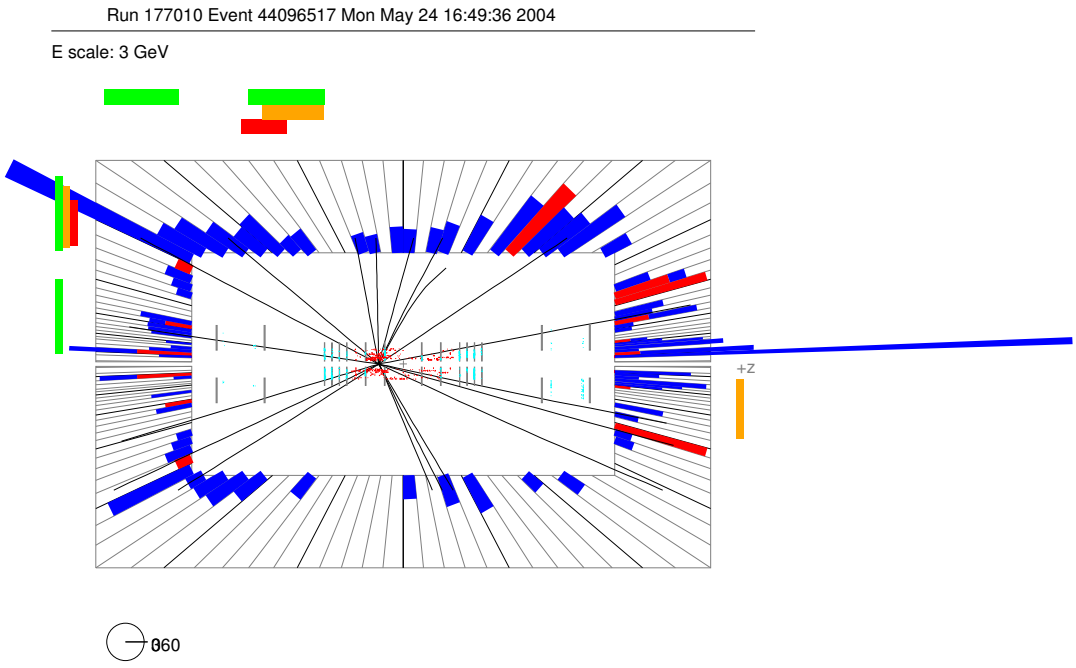

Figure 21: Event display of event 44096517 from run 177010.

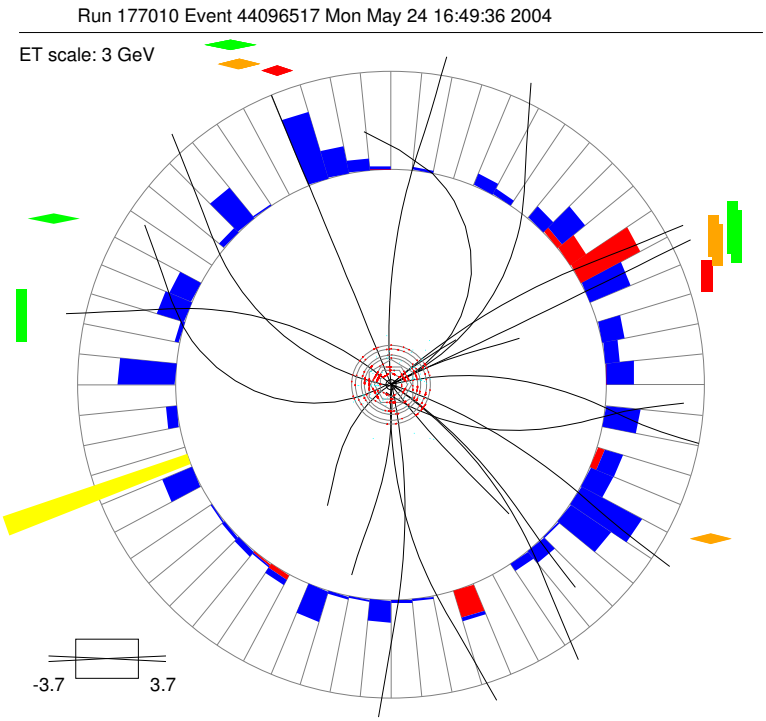

Figure 22: Event display of event 44096517 from run 177010.

8 Conclusions

We have performed a search for supersymmetry in the like-sign dimuon channel within the mSUGRA framework. We see data consistent with the expectation from background.

The Monte Carlo signal samples refer to points in mSUGRA parameter space which are not accessible within this channel by itself. We have combined our results with those from other channels.

A limit has been set on the total cross section for associated $\tilde{\chi}_1^{\pm}$ and $\tilde{\chi}_2^0$ production with leptonic final states. DØ Note 4368 has been posted, which summarizes this combination.

References

[1] H.E. Haber and G.L. Kane, Phys. Rep. **117**, 75 (1985).

[2] J. Nachtman, D. Saltzberg, and M. Worcester for the CDF collaboration, "Study of a Like-Sign Dilepton Search for Chargino-Neutralino Production at CDF", **hep-ex/9902010**, 1999.

[3] H.T Diehl, M. Arov, A. Askew, et al., " 'Ring-of-Welding' and Calorimeter Noise Characteristics," DØ Note 4286.

[4] Muon ID group p14 MuoCandidate web page,
"http://www-d0.fnal.gov/phys_id/muon_id/d0_private/certif/p14/index.html"

[5] NP group skimming web page,
"http://www-clued0.fnal.gov/ğusbroo/d0_private/skims-to-trees.html"

[6] CS group home page, "http://www-d0.fnal.gov/Run2Physics/cs/index.html"

[7] D. Whiteson and M. Kado, "Muon Isolation Studies", DØ Note 4070.

[8] S. Chakrabarti, private communication.

[9] W. Beenakker , M. Klasen , M. Krämer, T. Plehn, M. Spira and P.M. Zerwas, The Production of Charginos/Neutralinos and Sleptons at Hadron Colliders, **hep-ph/9906298**, 1999.